Mechanisms of separation of the elastic step and the thermal step

Seiji Miyashita*
JSR-UTokyo Collaboration Hub, CURIE, Department of Physics,
Graduate School of Science, University of Tokyo, Bunkyo-Ku, Tokyo, 113-0033, Japan

Masamichi Nishino†
Research Center for Materials Nanoarchitectonics,
National Institute for Materials Science, 1-1 Namiki,Tsukuba, Ibaraki 305-0044, Japan

Cristian Enachescu‡
Faculty of Physics, Alexandru Ioan Cuza University of Iasi, Iasi 700506, Romania
(Dated: December 9, 2024)

The elastic interaction causes a two-step conversion from the low-spin (LS) to the high-spin state (HS) following a femtosecond laser pulse excitation. These steps occur on different timescales: a spin conversion (elastic step) in a short time due to pressure propagation and a late spin conversion (thermal step) resulting from heat diffusion. In this paper, we provide a brief review of models for spin crossover phenomena, emphasizing the role of the difference of degeneracy of the HS state and LS state and elastic interaction due to changes in local structures. We also review theoretical approaches to these effects. Additionally, to analyze the dynamical process of spin conversion after photo-irradiation, it is necessary to consider mechanisms of heat transfer among spins. Recently, we proposed a two-temperature model that incorporates both lattice and spin temperatures, which enables us to reproduce the two steps under an early uniformization of the lattice temperature, highlighting the importance of the timescales of these processes. Furthermore, we explore possible mechanisms to separate the two steps by examining the different timescales of processes of spin conversions by mechanical and entropic forces, and also by considering changes of local temperature due to spin conversion.

I. INTRODUCTION

Spin-crossover (SC) phenomenon is a transition between bistable states, typically the high spin (HS) state and the low spin (LS) states [1]. Due to the difference in degeneracies of the LS and HS states, various interesting thermal processes emerge, including different forms of hysteresis. This phenomena have been analyzed by the so called Ising like model [2], where the effects of degeneracy are incorporated by introducing a temperature-dependent external field in the usual non-degenerate Ising model. The metastability of the phases results in a range of intriguing ordering processes [3–5].

Apart from the degeneracy difference, it has been noted out that the volume difference of the two states, or more generally difference of local lattice structure, causes deformation of the lattice. The elastic energy resulting from this deformation induces an effective interaction among the spin states [6–9]. This elastic interaction is responsible for the long range ferromagnetic interaction [10] which causes various interesting phenomena [11–18].

The elastic interaction plays a significant role not only in static thermodynamic properties but also in dynamics in ordering process. Recently, an intriguing dynamical ordering process following ultrafast photo-irradiation driven by the elastic interaction was observed [19]. Specifically, the high pressure due to the elastic force at the excited HS propagates in a short period corresponding to sound propagation, and expands the lattice, which causes an increase of HS fraction. This phenomenon is known as the "elastic step." This step occurs much before further increase of the HS fraction due to heating of the whole system due to photo-irradiation, referred to as the "thermal step." Consequently, two peaks appear in the HS fraction's evolution. This dynamical phenomenon is driven by propagation of elastic deformation and thermal diffusion [19, 20]. The appearance of these two peaks depends on the sample size. In a small system, the injected energy escapes to the thermal bath (sample environment) before the thermal step occurs, so only the elastic step is observed. while In a large sample, however both steps are observed.

*miyashita-seiji@g.ecc.u-tokyo.ac.jp@keio.jp
†NISHINO.Masamichi@nims.go.jp
‡cristian.enachescu@uaic.ro

One may attribute such separation to the properties of fast propagation of the elastic deformation and slow propagation of heat. To study this process of spin conversion with thermal diffusion, models of dynamic processes have been explored [20, 21]. Assuming that thermal diffusion is much slower compared to the pressure propagation, the temperature profile in the system becomes highly inhomogeneous in the process, which can cause the two steps in development of HS fraction. This model is called "single-temperature model". However, it has reported that the thermalization of the lattice is very fast [22] and uniformization of the temperature happens in a short time before the thermal step. In this context, a two-temperature model has been introduced, considering two types of temperatures: the lattice temperature and the spin temperature [21]. The former represents the energy of the total lattice vibration, while the latter corresponds to an energy responsible to the spin conversion.

To study these dynamical properties, detailed timescales of processes are important. In the present paper, we begin with a brief review on modeling of the spin crossover phenomena and explore modeling of the dynamics of processes. First, we consider the timescales of relaxation in both of the original degenerate model and the Ising-like model, finding that both yield the same thermodynamic properties. Next, we consider dynamical features of processes, such as the difference between the spin conversion process driven by a mechanical force (pressure) and that due to an entropic effect (difference of degeneracy). We also assess the effect of heat emission during the spin conversion. With these features in mind, we attempt to realize the two steps in a single-temperature model with rapid temperature uniformization.

II. MODELS

A. Ising-like model

As aforementioned, the degeneracy of the LS and HS states plays key role for the SC phenomena. The HS state has the energy D and degeneracy $n_{\rm HS}$ while the LS state has the energy $-D$ and degeneracy $n_{\rm LS}$. Electrical situations of the LS and HS are depicted in Fig. 1, where the difference of the spins is shown ($S_{\rm LS}=1/2$ and $S_{\rm HS}=5/2$ for the LS and HS states, respectively). It should be noted that the degeneracies $n_{\rm HS}$ and $n_{\rm LS}$ come from not only the spin state but also from the lattice degree of freedom. Therefore, the ratio $g=n_{\rm HS}/n_{\rm LS}$ is much larger than that of the spin part $g_{\rm spin}=(2S_{\rm HS}+1)/(2S_{\rm LS}+1)$. To treat the effect of degeneracy, the so-called Ising-like model has been introduced [2–

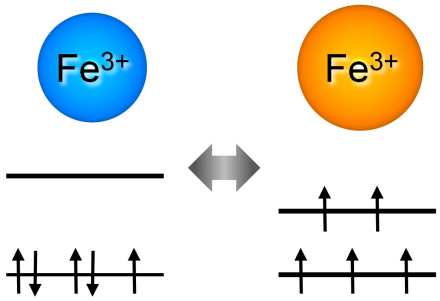

FIG. 1: Schematic picture of the LS and HS states of Fe^{3+} ion. (Courtesy of Professor Hiroko Tokoro)

4]. Let HS spin states of the ith ion be noted by $s_i=+1 (i=1,\cdots n_{\rm HS})$ and LS by $s_i=-1 (i=1,\cdots n_{\rm LS})$. Then, the partition function is given by

$$Z=\sum_{s_i=\underbrace{-1,\cdots,-1}_{n_{\rm LS}},\underbrace{1\cdots 1}_{n_{\rm HS}}}^{n} e^{-\beta E_i}=n_{\rm HS}e^{-\beta D}+n_{\rm LS}e^{\beta D}=\sqrt{n_{\rm HS}n_{\rm LS}}\left(\sqrt{\frac{n_{\rm LS}}{n_{\rm HS}}}e^{\beta D}+\sqrt{\frac{n_{\rm HS}}{n_{\rm HL}}}e^{-\beta D}\right)$$

$$=\sqrt{n_{\rm HS}n_{\rm LS}}\left(e^{\beta D-k_{\rm B}T\ln(n_{\rm HS}/n_{\rm LS}))/2}+e^{-\beta(D-k_{\rm B}T\ln(n_{\rm HS}/n_{\rm LS}))/2}\right)=\sum_{\sigma=\pm 1}e^{-\beta H_{\rm eff}\sigma}, \tag{1}$$

where

$$H_{\rm eff}=-D+\frac{1}{2}k_{\rm B}T\ln g, \quad g=\frac{n_{\rm HS}}{n_{\rm LS}}. \tag{2}$$

Thus, the original model with degenerate states is expressed by an Ising model ($\sigma = \pm 1$ without degeneracy) with the effective temperature-dependent field $H_{\rm eff}$. This transformation is also good even if the Hamiltonian contains interactions among spin states as explained in Computational Details Part A. Thus, models with interactions among spin states:

$$\mathcal{H}_{\rm Ising} = -J \sum_{<ij>} s_i s_j + D \sum_i s_i \tag{3}$$

is expressed by

$$\mathcal{H}_{\rm Ising} = -J \sum_{<ij>} \sigma_i \sigma_j - H_{\rm eff} \sum_i \sigma_i. \tag{4}$$

For the phase transitions of SC systems, the cooperative interaction is inevitable. The importance of the cooperativity among spins for the transition was pointed out from the experiments of the measurement of the heat capacity by Sorai and Seki, and they proposed the so-called domain model [23]. The relation between the domain model and the Ising-like model was clarified by a microscopic theoretical study [24]. This type of modeling is good for bistable systems with different degeneracies, i.e., not only for SC system but also charge transfer model and charge transfer SC model [25].

Thermal properties of the spin crossover model are obtained from the phase diagram (T, H) of corresponding Ising model [3, 4]. There appear several different types of ordering processes as depicted in Fig. 2, i.e., (I) smooth crossover, (II) smooth transition with low-temperature metastable HS phase, (III) first-order phase transition, (IV) first-order phase transition with low-temperature metastable HS phase, and (V) hidden LS phase. Temperature dependences of

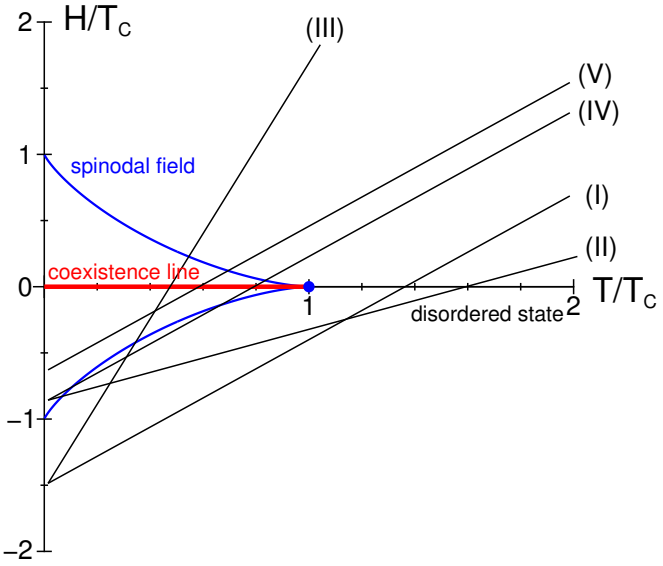

FIG. 2: Phase diagram of an Ising model and various cases of spin crossover system which are expressed by lines of the slope given by $\frac{1}{2}k_{\rm B}\ln\left(\frac{n_{\rm HS}}{n_{\rm LS}}\right)$.

HS fraction $f_{\rm HS}$

$$f_{\rm HS} = \frac{\langle \sigma_i \rangle + 1}{2} \tag{5}$$

to the Types I $\sim$ V are depicted in Fig. 3. One of characteristics of SC model is the so-called LIESST (light induced excited spin state transition) [26, 27]. That is, when the LS state is excited to HS state by an photo-irradiation, the excited HS state has a long lifetime. There may be two cases of LIESST. One of them is caused by long relaxation time

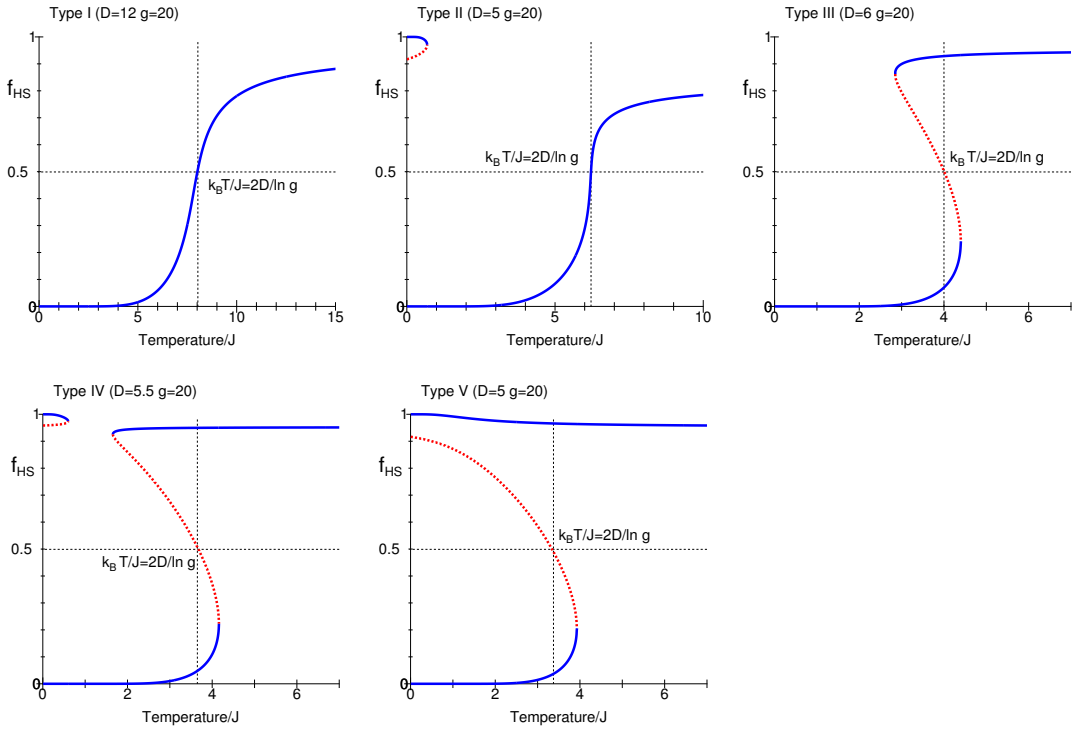

FIG. 3: Corresponding temperature dependence of HS fraction to Fig. 2.

at low temperatures where all the processes change very slowly. The other is the case where the HS state is trapped at the metastable branch in case IV. In this case $f_{\rm HS}$ first relaxes to the local stable value, although it finally relaxes to LS state after a long time. [27] Systematic changes from the type III to IV have been studied in $Rb_2Mn[Fe(CN)_6$ families, where the case (IV) was found in the experiments [28] and also the case (V) in the experiment [29]. When the interaction between the nearest neighbor sites is antiferromagnetic, the corresponding phase diagram of the Ising model becomes complicated and the SC ordering becomes two-step [30]. When the interactions become frustrated, e.g., the case in which signs of interactions of nearest neighbor and the next nearest neighbor pairs are different, two-step and more complicated ordering process appear which have been found in experiments [17, 31]

B. Models for elastic interaction

Elastic interaction has been recognized as an ingredient of the SC transition and lead to various interesting properties [32]. The volume, more generally local lattice structure, changes between the LS and HS states, and the change causes deformation of the lattice [6–9]. This deformation causes a long-range interaction among spins used the elastic energy of the lattice [10].

Here we briefly review models so for studied for the elastic interaction in spin-crossover systems.

1. Model A

The elastic interaction was firstly studied by the model A explained below. In the model, motions of quantities are treated by a molecular-dynamics simulation with Nose-Hoover thermostat [6, 33]. This model is suitable to reproduce various dynamical properties.

$$\mathcal{H}_{\rm A} = \sum_i^N \frac{\boldsymbol{P}_i^2}{2M} + \sum_i^N \frac{p_i^2}{2m} + \sum_i^N V_i^{\rm intra}(r_i) + \sum_{<ij>} V_{ij}^{\rm inter}(\boldsymbol{X}_i, \boldsymbol{Y}_j, r_i, r_j). \tag{6}$$

Here, the position and the momentum of the i-th molecule are given by $(\boldsymbol{X}_i, \boldsymbol{P}_i)$. The coordinate (molecular radius) and the corresponding momentum representing the intra-molecular motion (breathing mode) are denoted by (r_i, p_i).

The elastic interaction among molecules forming a lattice structure (Fig. 4) is given by the excess energy due to deformation of nearest neighbor pairs

$$V_{ij}^{\rm inter}(\boldsymbol{X}_i, \boldsymbol{Y}_j, r_i, r_j) = f(d_{ij}), \tag{7}$$

where $f(x)$ is a function of the distance between molecules $d_{ij} = |\boldsymbol{X}_i - \boldsymbol{X}_j| - (r_i + r_j)$. The concrete form which was used in the paper [6] has the form $f(x) = D\left(e^{a'(x-x_0)} + e^{-b'(x-x_0)}\right)$ with $a' = 0.5$ and $b' = 1.0$. The value x_0 is chosen to make $f(x)$ have the minimum at $x = 0$. An alternate form of $f(x)$ could be the form of $\mathcal{H}_{\rm lattice}$ (13) given below.

To keep the lattice to be a not titled square shape, we include interaction between the next nearest neighbor (nnn) pairs in addition, which is small compared to that of the nearest neighbor. If we use the triangular lattice, we do not need the nnn interaction.

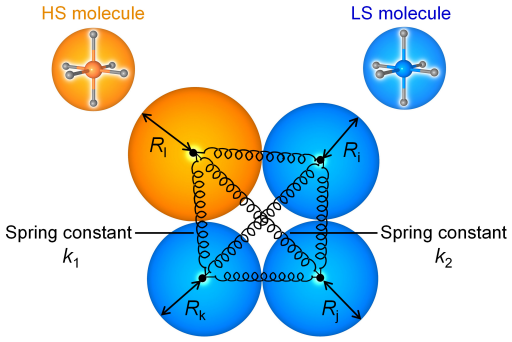

FIG. 4: Elastic interaction $V_{ij}^{\rm inter}(\boldsymbol{X}_i, \boldsymbol{Y}_j, r_i, r_j)$ among molecules (Courtesy of Professor Hiroko Tokoro).

The energy for the internal degree of freedom is given by $V_i^{\rm intra}(r_i)$ as a function of the radius of the molecule r_i. The effective potential energy for the radius r_i, $V_i^{\rm intra}(r_i)$, is given by an bistable form depicted in Fig. 5. Representing the differences of energies and of degeneracies, the potential energies for the LS and HS states are given by harmonic potentials by

$$V_{\rm LS} = \frac{1}{2}a_{\rm LS}(r_i - r_{\rm LS})^2, \quad V_{\rm HS} = \frac{1}{2}a_{\rm HS}(r_i - r_{\rm HS})^2 + 2D, \tag{8}$$

respectively. The coefficients $a_{\rm LS}$ and $a_{\rm HS}$ are taken to be proportional to the stiffness constants of breathing modes of the LS and HS states, respectively. We assume that the potential energies are hybridized by a mixing term J, and then the hybridized potential energy E is given by

$$\begin{vmatrix} V_{\rm LS} - E & J \\ J & V_{\rm HS} - E \end{vmatrix} = 0, \tag{9}$$

which gives

$$E_\pm = \frac{V_{\rm LS} + V_{\rm HS} \pm \sqrt{4J^2 + (V_{\rm HS} - V_{\rm LS})^2}}{2}. \tag{10}$$

These energies are depicted in Fig. 5. In actual spin-crossover materials, there exists a large entropy difference between the LS and HS states. As mentioned, it should be noted that the degeneracies $n_{\rm LS}$ and $n_{\rm HS}$ come from not only the spin part but also contributions from surrounding ligands. To treat such large entropy difference in the molecular dynamics model (6), an oscillator coupling to the spin state in each molecule was introduced, in which the frequency of the oscillator varies depending on the spin state [6]. To control temperature and/or pressure, Nose-Hoover thermal bath and/or Andersen pressure bath were used [6] . With this modeling, various peculiar phenomena due to the elastic interactions, e.g., macroscopic nucleation phenomena [11], have been studied. This model is suitable to study effects of mechanical dynamics at zero and finite temperatures because the motion is given by molecular dynamics.

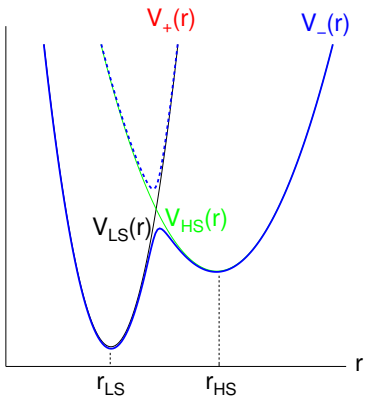

FIG. 5: Schematic picture of the potential energies $V_{\rm LS}$ (black), $V_{\rm HS}$ (green), V_+ (blue, dash), and V_- (blue, solid). V_- is used for $V_i^{\rm intra}(r_i)$.

2. *Model B*

In the model B, the motions of both spin and lattice are given by transition probabilities with the detailed balance [7]. In this model, the energy of the positions ($\{\boldsymbol{X}_i\}$) and the spin states $\{\sigma_i\}$ is given by

$$\mathcal{H}_{\rm B} = \mathcal{H}_{\rm spin} + \mathcal{H}_{\rm lattice}. \tag{11}$$

The spin part is

$$\mathcal{H}_{\rm spin} = \sum_i \left(D - \frac{1}{2} k_{\rm B} T \ln g \right) \sigma_i, \quad g = \frac{n_{\rm HS}}{n_{\rm LS}}, \tag{12}$$

and the lattice part is

$$\mathcal{H}_{\rm lattice} = \frac{1}{2} \sum_{<ij>} k_1 \left(|\boldsymbol{X}_i - \boldsymbol{X}_j| - R(\sigma_i) - R(\sigma_i) \right)^2 + \frac{1}{2} \sum_{<il>} k_2 \left(|\boldsymbol{X}_i - \boldsymbol{X}_l| - \sqrt{2}(R(\sigma_i) + R(\sigma_j)) \right)^2, \tag{13}$$

where $< ij >$ denotes all the nearest neighbor pairs and $< il >$ the next nearest neighbor pairs in a square lattice as depicted in Fig. 4. Here, the second term is introduced to keep the lattice to be square shape. Thus, k_2 is set to be small compared to k_1. $R(\sigma)$ denotes the radius of the molecule of the spin state of σ. In the model B, both the motion of position (lattice) and the change of spin state are treated by transition probabilities (i.e., as usual Monte Carlo methods). By this model, various interesting properties due to elastic interaction have been studied. For example, the mean-field type long-range ferromagnetic interaction among spins [10], distribution of local stress [13], a complicated phase diagram due to competition between a short-range antiferromagnetic interaction and the long-range interaction due the elastic model [14–16], and multistep transitions [17].

Furthermore, this model can be applied to study dynamical properties. Using different timescales for the spin-state conversion by MC and lattice motion by MD, it was shown that the nature of interface growth (domain wall propagation) varies depending on the relative timescales [12].

3. *Model C*

Thermo-mechano-elastic method proposed by Enachescu consists of over-damped lattice dynamics and thermal conversion of spins [8]. In this model, the positions of the molecules evolve according to the equation:

$$m \frac{d^2 \boldsymbol{X}_i}{dt^2} = \boldsymbol{F}_i - \mu \frac{d\boldsymbol{X}_i}{dt}, \tag{14}$$

where μ is a damping constant. This equation brings the system to the low energy state. Because of the friction, in a long time, the state reaches the ground state (or at least local minimum state) and the motion does not take

the temperature effect onto account. But, when the mass of molecules is large, it gives a good description of lattice motion. Also, for practical calculation, the lattice dynamics is performed in a finite time and the lattice state does not go to the minimum energy position. To improve this point, one may use the Nose-Hoover formalism [33, 34] or introducing a noise to realize the equilibrium state by the fluctuation and dissipation relation [35]. For the spin conversion, Monte Carlo update with the following transition probability is used:

$$\begin{aligned} P^i_{\mathrm{HS}\to\mathrm{LS}} &= \tfrac{1}{\tau}\exp\left(-\frac{E_A-\kappa p_i}{k_{\mathrm{B}}T}\right), \\ P^i_{\mathrm{LS}\to\mathrm{HS}} &= \tfrac{1}{\tau}\exp\left(-\frac{E_A+\kappa p_i}{k_{\mathrm{B}}T}\right)\exp\left(-\frac{D-k_{\mathrm{B}}T\ln g}{k_{\mathrm{B}}T}\right), \end{aligned} \tag{15}$$

where p_i is the sum of the pressures from the neighboring sites to the ith molecule. In the triangular lattice, we consider only nearest neighbor pairs, and the elastic interaction and the force are given by

$$\mathcal{H}_{\mathrm{latice}} = \frac{1}{2}k\delta x_{ij}^2, \quad \boldsymbol{F} = -k\delta x_{ij}, \tag{16}$$

where δx_{ij} is a change of the distance from the equilibrium length. Then the pressure is given by

$$p_i = \sum_{j:\text{neighboring sites}} k\delta x_{ij}. \tag{17}$$

The relation between models B and C has been studied in Ref. [9]. This model has been applied for several SC phenomena, e.g., photo-thermal swotching [18, 20, 21]. Using over-damped lattice motion in Model B is physically equivalent to Model C. In our previous papers, we utilized Model C; however, in the present paper, we employ Model B with over-damped lattice motion, which produces qualitatively (and almost quantitatively) the same results as those obtained from Model C.

C. Models for dynamics after ultrafast pulse photo-irradiation

To study mechanism of the elastic and thermal steps after ultrafast pulse photo-irradiation, models with thermal conduction is necessary. Here, we review models so far studied.

It should be noted that in the simulation, the Hamiltonian (11) is only for the potential energy which consists of the spin part (12) and elastic part (13). In classical systems, the kinetic part is independent of the potential part. The temperature somehow represents kinetic energy, and the transfer of kinetic energy is treated by the heat transfer which is not included in the Hamiltonian. To study dynamics of systems with non-uniform temperatures, we need some heat transfer equation in addition to the Hamiltonian, which will be explained in the following subsections.

1. Single-temperature model

In this model, we consider a local temperature, $T_{\mathrm{L}}(\boldsymbol{x},t)$, for a molecule at a position $\boldsymbol{x}$ at a time t. Providing heat transfer between neighboring sites and also heat escape to external thermal bath with the temperature T_{bath}, the time evolution of the local temperature, $\{T_{\mathrm{L}}(\boldsymbol{x},t)\}$ is given by

$$T_{\mathrm{L}}(\boldsymbol{x},t+\Delta t) = T_{\mathrm{L}}(\boldsymbol{x},t) + \Delta t\left[\lambda\sum_{nn:\boldsymbol{x}'}\left(T(\boldsymbol{x}',t)-T(\boldsymbol{x},t)\right)+\kappa\sum_{\boldsymbol{x}}\left(T_{\mathrm{bath}}-T(\boldsymbol{x},t)\right)\right], \tag{18}$$

where λ gives the rate of energy diffusion to the neighboring sites, κ is the rate of heat escape to the external thermal bath. The unit of λ and κ is 1/MCS. In the present study, we demonstrate qualitative features of the processes, and thus here we choose the parameters to reproduce phenomena with typical features. In this respect, we study models in two dimensions. Real systems are in three dimensions where we must consider the inhomogeneous irradiation from the surface to the bulk, which is not considered in the present paper although it was studied the previous papers [20, 21].

In the present paper, we use the following parameters: The lattice is a 60×60 square lattice, and $D = 1064$K, $g = 1069$, $k_1 = 80000\mathrm{K/nm}^2$, $k_2 = 8000\mathrm{K/nm}^2$ (the equilibrium distance $r_{\mathrm{LS}} = R(-1) = 1$ and the length is measured by the unit nm), and the bath temperature $T_{\mathrm{bath}} = 280K$. In Fig. 6, we show the temperature dependence of f_{HS} in the present model with the parameters. In the present study, $2D/k_{\mathrm{B}}\ln g \simeq 305$, the bath temperature is $T_{\mathrm{bath}} = 280$K

which is set just below the hysteresis loop. The average temperature $T_{\rm all}$ just after the irradiation with $T_{\rm EX} = 480$K is given by

$$T_{\rm all} = T_{\rm bath} \times 0.77 + T_{\rm EX} \times 0.23 \simeq 326{\rm K}. \tag{19}$$

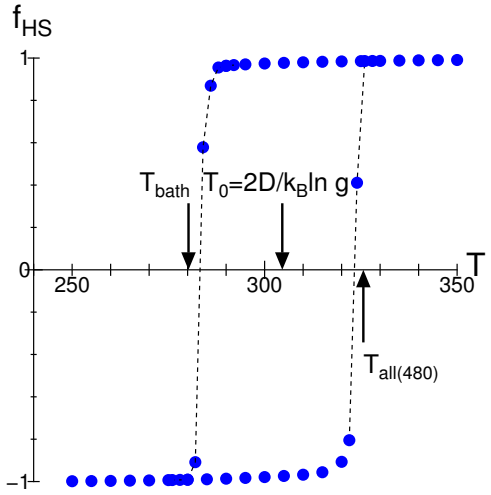

FIG. 6: Temperature dependence of $f_{\rm HS}$ of the present model.

Here, we consider the following processes after photo-irradiation. Before the photo-irradiation, the system is in equilibrium at a temperature $T_{\rm bath}$ which is just below the coexistence (hysteresis) region and the spins are in LS state. At the irradiation, some of molecules are excited and the local temperature increases to $T_{\rm EX}$ as shown in Fig. 7.

FIG. 7: (left) Before the photo-irradiation where almost all the local sites are in LS state (dark blue), and (right) a molecule (yellow) is excited by the photo irradiation.

We consider a case in which some of molecules are excited. Because the excited molecules tend to expand to the size of HS state, very high pressure is placed on the neighboring sites. Microscopically, the Fe-ligand distance increases in an excited molecule, but the volume (lattice parameter) of the whole system is little changed immediately after irradiation. Thus, the high pressure is applied to the neighboring molecules. In the present paper, we do not refer to the details of this fast process although it is important as a microscopic process.

The energy diffuses to the neighboring sites, and the temperature of the irradiated site decreases heating up the neighboring sites (Fig. 8(a)). In this process, some of the irradiated sites are pushed back to LS state (Fig. 8(b)) due to the high pressure, and the number of HS molecules decreases just after the irradiation. When the excited spin keeps HS state, high pressure remains, and the high pressure propagates over the system and the size of system expands. This expansion of the system causes reduction of the pressure, and makes the molecules to convert to HS, which makes an increase of the HS fraction. When the energy transfer is slow, after the increase the number of HS molecules decreases because the decrease of the excited HS molecules, which makes a peak of HS fraction. These processes give the elastic step. This step occurs at the timescale of pressure propagation (an order of the sound velocity which is an order of few nano second). After a long time (in timescale of heat diffusion of an order of μs), temperatures of all the sites become higher than the conversion temperature, and all the sites tend to become HS state, which is the thermal

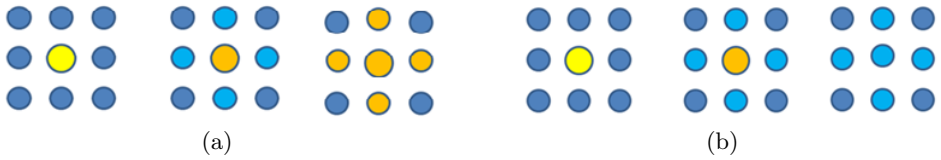

(a) (b)

FIG. 8: (a) Conversion neighboring sites to HS state (orange), and (b) a case where the excited site is pushed back to LS state with high energy (right blue).

step. After much longer time, energy escapes to the external thermal bath, and the temperature comes back to the original one of the LS state where almost all the spins convert to LS again. Like Fig. 2 of Ref. [21] obtained by the model C, we show an example of such process in Fig. 9. Time dependence of $n_{\rm HS}$ (HS fraction) is depicted in Fig. 9. Lower panel shows $n_{\rm HS}$ in logarithmic time. The change at the irradiation occurs at $t = 100$ which is very close to the left axis in the upper panel. The resulting state depends on parameters of excitation, heat transfers, and the heat leaking to the bath. By choosing an appropriate set of parameters, we can reproduce the two steps similarly to that observed experiment [19].

In the figure, we also plot time dependence of the quantities "vol(t)/vol(0)", $a(t)/a(0)$, $10 \times \Delta a/a(0)$ and $5 \times E(t) - E(0)/E(0)$. To see the change clearly, multiplied values are plotted. "vol" is the volume (area) of the lattice and vol(0) is the value in the LS state, and a is the average distance of the neighboring sites i and j, $\sqrt{\langle(|\boldsymbol{X}_i - \boldsymbol{X}_j|^2\rangle}$, $\Delta a/a(0) = (a(t) - a(0))/a(0))$ and E is the sum of local temperature of the current configuration. In Computational Details Part B, a vs $n_{\rm HS}$ is plotted in Fig. 15.

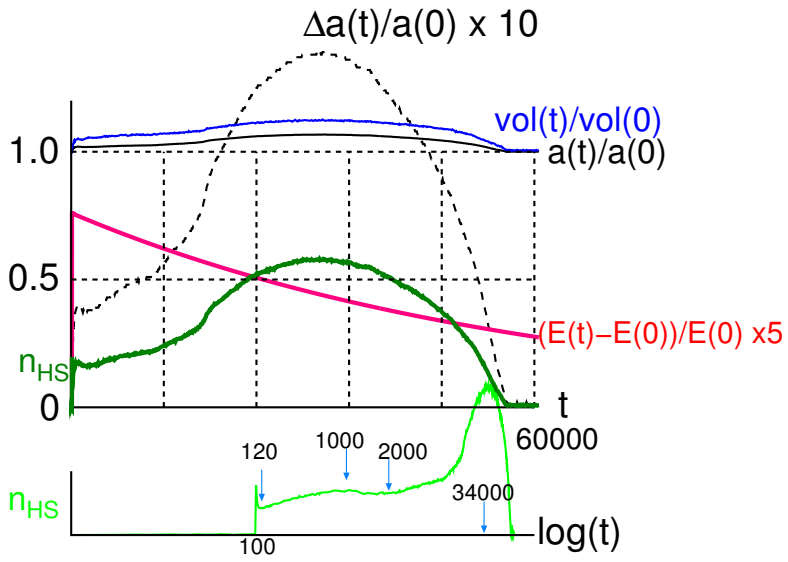

FIG. 9: Example of two steps in a single-temperature model with $r_{HS}/r_{\rm LS} = 1.102$, $\lambda = 0.0002$, and $\kappa = 0.000017$ in a two-dimensional system with 60×60 sites. "vol" is the volume of the lattice, E the total energy, "a" the average lattice constant and $n_{\rm HS}$ is HS fraction. The lower panel shows $n_{\rm HS}$ in the logarithmic time. Temperature of the irradiated site is $T_{\rm EX} = 480$K, and the probability of irradiated sites is $p = 0.23$.

However, it is found that the spin configuration is very inhomogeneous as depicted in Fig, 10 similarly to Fig. 2 (right) of Ref. [21]. This inhomogeneity of local temperature contradicts experimental observation that the thermalization of the lattice is very fast around 10ns which is about the time of elastic step [22]. They found that the dynamics span from subpicosecond molecular photo switching followed by volume expansion (on a nanosecond timescale) and additional thermal switching (on a microsecond timescale) from results of time-resolved X-ray diffraction. Therefore, uniformization of the temperature should be achieved much before the thermal step.

If λ is large, local temperature becomes uniform fast, but the dominant spin conversions are given by thermal conversion (i.e., thermal step), and the elastic step does not appear.

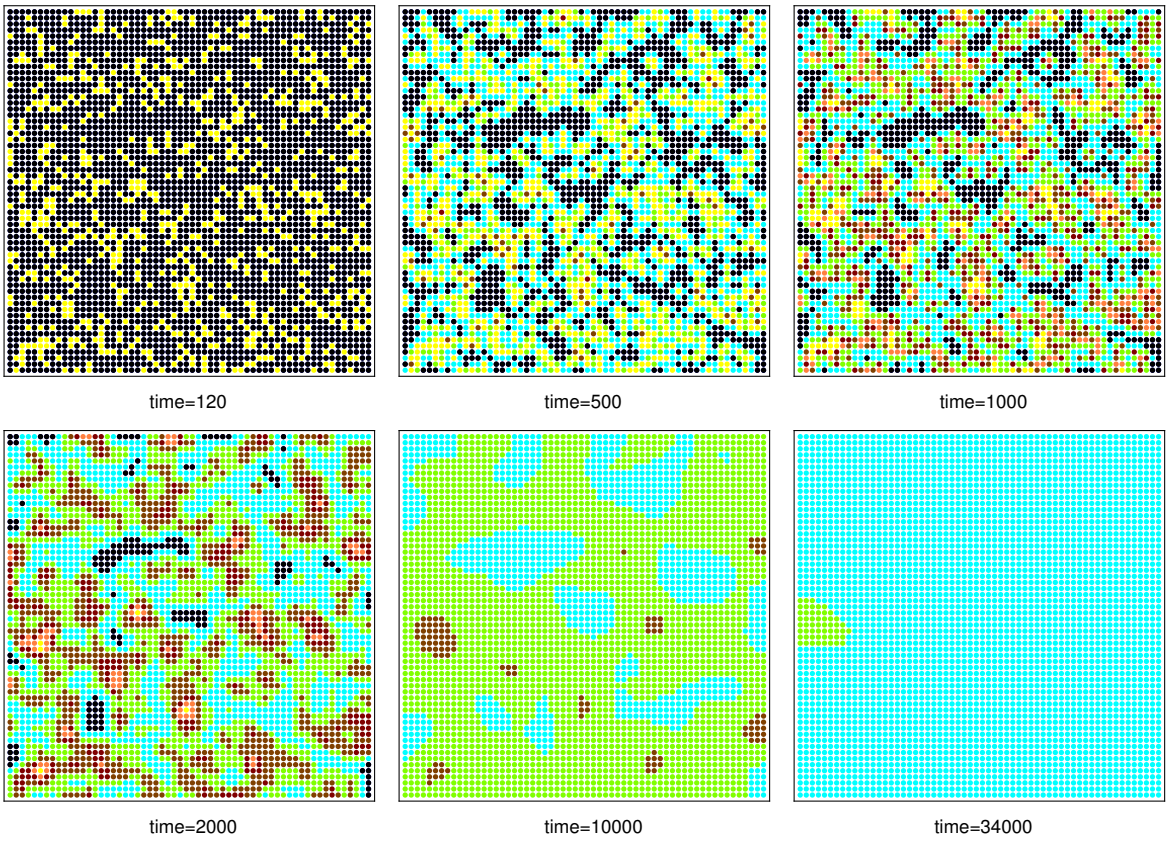

FIG. 10: Spin configurations at times. The colors denote different temperatures: yellow : $T \geq 390$, orange: $390 > T \geq 370$, dark brown: $370 > T \geq 350$, light brawn: $350 > T \geq 330$ green : $330 > T \geq 310$, light blue: $310 > T \geq 290$, dark blue : $290 > T \geq 280$, black : $280 > T$.

2. *Two-temperature model*

To overcome this difficulty, we introduced a two-temperature model [21]. In this model, we consider two kinds of temperatures, i.e., the lattice temperature $T_{\rm L}(\boldsymbol{x}, t)$ which expresses the total energy at a molecule at a position $\boldsymbol{x}$ at a time t and the spin temperature $T_{\rm S}(\boldsymbol{x}, t)$ which is responsible for the spin conversion. The temperatures follw the following equations:

$$T_{\rm L}(\boldsymbol{x}, t+\Delta t) = T_{\rm L}(\boldsymbol{x}, t) + \Delta t \left[\lambda \sum_{nn:\boldsymbol{x}'} \left(T_{\rm L}(\boldsymbol{x}', t) - T_{\rm L}(\boldsymbol{x}, t) \right) + \kappa \sum_{\boldsymbol{x}} \left(T_{\rm bath} - T_{\rm L}(\boldsymbol{x}, t) \right), \right] \tag{20}$$

and

$$T_{\rm S}(\boldsymbol{x}, t+\Delta t) = T_{\rm S}(\boldsymbol{x}, t) + \Delta t \lambda' \sum_{\boldsymbol{x}} \left(T_{\rm L}(\boldsymbol{x}, t) - T_{\rm S}(\boldsymbol{x}, t) \right), \tag{21}$$

where λ gives the rate of energy diffusion to the neighboring sites, κ is the rate of heat escape to the external thermal bath, and λ' is the rate of conversion from the lattice temperature to the spin temperature. In our recent paper [21], we used slightly different model. But here we use this model which is based on essentially the same picture.

We assume the spin state at each site is given by the equilibrium state with its spin temperature. Here we assume that $\lambda \gg \lambda'$, so that the energy diffuses rapidly, and the spin temperature comes close to the lattice temperature rather slowly. The escape rate to the external bath κ is assumed to be much smaller than λ'. In this case, the lattice temperatures become uniform in a short time, while the spin temperature remains inhomogeneous. And thus, tuning these parameters, we can produce the elastic step and thermal step, separately in almost uniform lattice temperatures [21]. A two-step of HS fraction is depicted in Fig. 11 which corresponds to Fig. 3 in our recent paper [21]. In the following section, we consider properties of the timescales of spin conversion in various cases.

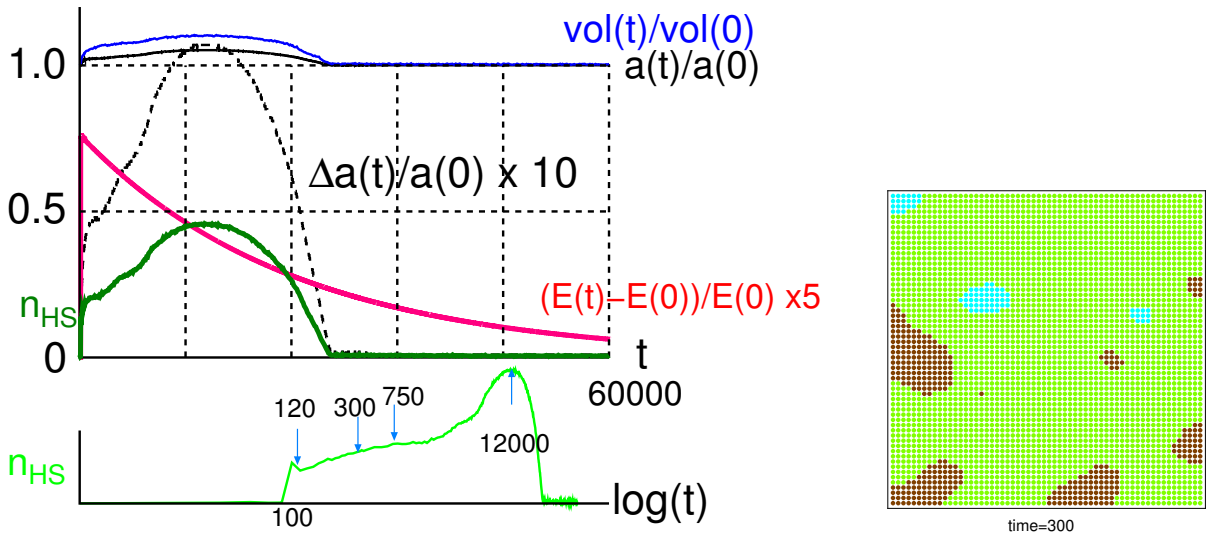

(a) (b)

FIG. 11: (a)Example of two steps in a two-temperature model with $r_{HS}/r_{\rm LS} = 1.1$, $\lambda = 0.02$, $\lambda_{\rm S} = 0.001$and $\kappa = 0.00005$ in a two-dimensional system with 60×60 sites. The notations are the same in Fig. 9. (b) Profile of the lattice temperature at the time $t = 300$ denoted by the arrow in (a). The temperature of the irradiated site is $T_{\rm EX} = 480$K, and the probability of irradiated sites is $p = 0.23$.

III. TIMESCALES OF PROCESSES

Now we consider the timescales of processes. For thermodynamics, the timescales of relaxation process are not important. But for dynamical properties, the timescales have crucial role. Here we consider the following points
(1) timescales of the degeneracy model and the Ising-like model,
(2) timescales of thermal process and mechanical process,
(3) timescales of heat emission to the local bath in mechanical spin-conversion process.

A. Timescales of the degeneracy model and the Ising-like model

Let us begin with (1) timescales of the degeneracy model and the Ising-like model. For spin-crossover phenomena, the degeneracy, i.e., the difference of degeneracy of the LS and HS states is important. For equilibrium thermodynamic properties, the effect of the different degeneracies can be expressed by an effective temperature dependent field (2).

At high temperatures, the system tends to be HS state because of the entropy effect, i.e., $n_{\rm HS} > n_{\rm LS}$ as depicted in Fig. 12(left). In the Ising-like model, the effective field (2) becomes positive and the energy of HS state in the Ising-like model becomes lower as depicted in Fig. 12(right). These two pictures have the same thermodynamic properties because their partition functions are the same.

Now we study dynamical properties of the models. In particular, we obtain the relaxation rates of both models in Monte Carlo simulations which give qualitative nature of relaxations.

Dynamics of Monte Carlo simulations are given by the so-called master equation which is equation of motion of the probability distribution updated by the transition probabilities among the states. Giving the transition probability per a unit time from the state i to j by $\{w_{i\to j}\}$, the master equation is given by

$$P(i,t+\Delta t) = P(i,t) - \Delta t \sum_{j\neq i}^{n} w_{i\to j} P(i,t) + \Delta t \sum_{j\neq i}^{n} w_{j\to i} P(j,t), \quad i = 1, \cdots, M. \tag{22}$$

Expressing the probabilities as a vector $\boldsymbol{P}(t)$, the master equation is given by in a matrix form with the time evolution

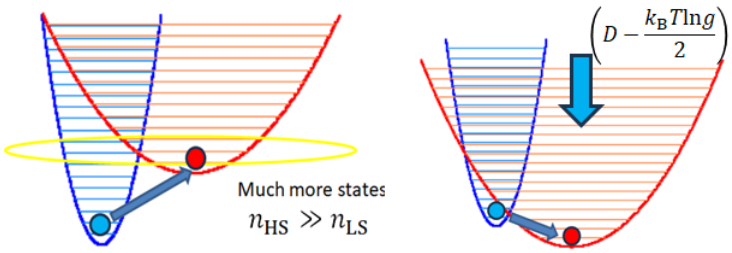

FIG. 12: (left)Comparison of spin conversion in the original degenerate model, and (right) that in the Ising-like model.

operator $\mathcal{L}$:

$$\begin{pmatrix} P(1,t+\Delta t) \\ P(2,t+\Delta t) \\ \vdots \\ P(M,t+\Delta t) \end{pmatrix} = \begin{pmatrix} w_{1\to1} & w_{2\to1}\Delta t\cdots & w_{M\to1}\Delta t \\ w_{1\to2}\Delta t & w_{2\to2} & \cdots & w_{M\to2}\Delta t \\ \vdots & \vdots & \ddots & \vdots \\ w_{1\to M}\Delta t & w_{2\to M}\Delta t & \cdots & w_{M\to M} \end{pmatrix} \begin{pmatrix} P(1,t) \\ P(2,t) \\ \vdots \\ P(M,t) \end{pmatrix} \to \boldsymbol{P}(t+\Delta t) = \mathcal{L}\boldsymbol{P}(t), \quad (23)$$

Here, we assume the detailed balance among the transition probabilities to realize the thermal equilibrium state:

$$\frac{w_{i\to j}}{w_{j\to i}} = \frac{P_{\mathrm{eq}}(j)}{P_{\mathrm{eq}}(i)}. \quad (24)$$

In the present study, we adopt the choice of Glauber type transition probability for each spin:

$$w_{i\to j} \propto e^{-\beta E_j}, \quad \beta = \frac{1}{k_{\mathrm{B}}T}, \quad (25)$$

and

$$w_{i\to i} = 1 - \sum_{i\neq j}^{M} w_{i\to j}\Delta t. \quad (26)$$

In the model with explicit degeneracies, the energy difference of the LS and HS states is $2D$, and energetically LS is favorable. But because n_{HS} is much larger than n_{LS}, HS state is realized at high temperatures. In the Ising-like model, the variable σ_i just takes ±1, but the effective energy includes the degeneracy effect as the temperature dependent field (2). And thus, HS state is realized at high temperatures. These processes are different, and we need to check the difference in dynamics. . The time-evolution operator for the degenerate model is expressed by a master equation is given by an $n \times n$ matrix, where $n = n_{\mathrm{HS}} + n_{\mathrm{LS}}$, while that of the Ising-like model is a 2×2 matrix. The relaxation rate is obtained from the eigenvalues of the matrices.

1. *Timescales of the degeneracy model*

The time evolution operator for a step of Δt in the original degenerate model is given by

$$\boldsymbol{P}(t+\Delta t) = \mathcal{L}\boldsymbol{P}(t) = \begin{pmatrix} \alpha & \beta & \cdots & & \beta & \gamma' & \cdots & \gamma' \\ \beta & \alpha & & & \vdots & \vdots & & \vdots \\ \vdots & \vdots & \ddots & & & & & \\ & \vdots & & \ddots & \beta & \vdots & & \vdots \\ \beta & \beta & & \beta & \alpha & \gamma' & \cdots & \gamma' \\ \gamma & \cdots & & & \gamma & \alpha' & \cdots & \beta' \\ \vdots & & & & & \vdots & & \vdots \\ \gamma & \cdots & & \cdots & \gamma & \beta' & \cdots & \alpha' \end{pmatrix} \begin{pmatrix} p_1 \\ \vdots \\ \vdots \\ p_{n_{\mathrm{HS}}} \\ q_1 \\ \vdots \\ \vdots \\ q_{n_{\mathrm{LS}}} \end{pmatrix}, \quad (27)$$

where

$$\beta = w_{\mathrm{HS}\to\mathrm{HS}} = \frac{1}{\tau_{\mathrm{HH}}}\Delta t, \quad \gamma = w_{\mathrm{HS}\to\mathrm{LS}} = \frac{1}{\tau_{\mathrm{HL}}} e^{D/k_{\mathrm{B}}T}\Delta t, \tag{28}$$

$$\beta' = w_{\mathrm{LS}\to\mathrm{LS}} = \frac{1}{\tau_{\mathrm{LL}}}\Delta t, \quad \gamma' = w_{\mathrm{LS}\to\mathrm{HS}}\frac{1}{\tau_{\mathrm{LH}}} e^{-D/k_{\mathrm{B}}T}\Delta t, \tag{29}$$

$$\alpha = 1 - \sum_{j\neq i} w_{1\to j} = 1 - (n_{\mathrm{HS}} - 1)\beta - n_{\mathrm{LS}}\gamma, \quad (i \leq n_{\mathrm{HS}}), \tag{30}$$

and

$$\alpha' = 1 - \sum_{j\neq i} w_{1\to j} = 1 - (n_{\mathrm{LS}} - 1)\beta' - n_{\mathrm{HS}}\gamma' \quad (n_{\mathrm{HS}} < i \leq n). \tag{31}$$

Here we assume

$$\tau_{\mathrm{LH}} = \tau_{\mathrm{HL}} = \tau_{\mathrm{X}}. \tag{32}$$

Now we obtain eigenstates and eigenvalues. In general, one of the eigenstates of the time evolution operator $\mathcal{L}$ represents the steady (equilibrium) state with the eigenvalue $\lambda_0 = 1$, and other eigenstates correspond to relaxation modes with the eigenvalues $\lambda_i < 1$ $(i = 1, 2, \cdots M-1)$ where $M = n_{\mathrm{HS}} + n_{\mathrm{LS}}$ is the dimension of the time evolution operator $\mathcal{L}$.

From the symmetry of the matrix $\mathcal{L}$, first, we consider a uniform state in which all the HS states are uniformly populated with a probability p and all the LS states are uniformly populated with a probability q:

$$\begin{pmatrix} p_1 \\ \vdots \\ \vdots \\ p_{n_{\mathrm{HS}}} \\ q_1 \\ \vdots \\ \vdots \\ q_{\mathrm{LS}} \end{pmatrix} = \begin{pmatrix} p \\ \vdots \\ \vdots \\ p \\ q \\ \vdots \\ \vdots \\ q \end{pmatrix}. \tag{33}$$

In this case, the eigenvalue equation with the eigenvalue λ is given by

$$p(\alpha + (n_{\mathrm{HS}} - 1)\beta) + qn_{\mathrm{LS}}\gamma' = \lambda p, \quad q(\alpha' + (n_{\mathrm{LS}} - 1)\beta') + pn_{\mathrm{HS}}\gamma = \lambda q. \tag{34}$$

Substituting (30) and (31), we have the relations:

$$p(1 - n_{\mathrm{LS}}\gamma) + qn_{\mathrm{LS}}\gamma' = \lambda p, \quad q(1 - n_{\mathrm{HS}}\gamma') + pn_{\mathrm{HS}}\gamma = \lambda q. \tag{35}$$

Thus, the λ is given by

$$\begin{vmatrix} 1 - n_{\mathrm{LS}}\gamma - \lambda & n_{\mathrm{LS}}\gamma' \\ n_{\mathrm{HS}}\gamma & 1 - n_{\mathrm{HS}}\gamma' - \lambda \end{vmatrix} = 0 \to (\lambda - 1)(\lambda - (1 - n_{\mathrm{LS}}\gamma - n_{\mathrm{HS}}\gamma')) = 0. \tag{36}$$

The eigenvalues are

$$\lambda_0 = 1, \quad \lambda_1 = 1 - n_{\mathrm{LS}}\gamma - n_{\mathrm{HS}}\gamma' = 1 - n_{\mathrm{LS}}\frac{1}{\tau_{\mathrm{X}}} e^{D/k_{\mathrm{B}}T}\Delta t - n_{\mathrm{HS}}\frac{1}{\tau_{\mathrm{X}}} e^{-D/k_{\mathrm{B}}T}\Delta t = 1 - \frac{\Delta t}{\tau_{\mathrm{X}}}\left(n_{\mathrm{LS}} e^{D/k_{\mathrm{B}}T} + n_{\mathrm{HS}} e^{-D/k_{\mathrm{B}}T}\right). \tag{37}$$

The eigenvalue λ_0 is for equilibrium state and the eigenvalue λ_1 gives the relaxation time.

$$(\lambda_1)^n = e^{-t/\tau}, \quad t = n\Delta t, \to \frac{1}{\tau} = -\frac{\ln \lambda_1}{\Delta t} \tag{38}$$

$$= -\frac{1}{\Delta t}\ln\left(1-\frac{\Delta t}{\tau_{\rm X}}\left(n_{\rm LS}e^{D/k_{\rm B}T}+n_{\rm HS}e^{-D/k_{\rm B}T}\right)\right) \simeq \frac{1}{\tau_{\rm X}}\left(n_{\rm LS}e^{D/k_{\rm B}T}+n_{\rm HS}e^{-D/k_{\rm B}T}\right). \tag{39}$$

The ration of p and q for the case of $\lambda_0 = 1$ is given by

$$-pn_{\rm LS}\gamma + qn_{\rm LS}\gamma' = 0 \to p = \frac{\gamma'}{\gamma}q \to p : q = n_{\rm HS}e^{-D/k_{\rm B}T} : n_{\rm LS}e^{D/k_{\rm B}T}. \tag{40}$$

This gives the equilibrium state which corresponds to the canonical distribution.

The ration of p and q for the case of $\lambda = 1 - n_{\rm LS}\gamma - n_{\rm HS}\gamma'$ is given by

$$pn_{\rm HS} + qn_{\rm LS} = 0 \to p = -\frac{n_{\rm LS}}{n_{\rm HS}}q. \tag{41}$$

The sum of all the components of $\boldsymbol{P}_1$ is zero ($pn_{\rm HS} + qn_{\rm LS} = 0$), which indicates that its eigenstate gives a relaxation mode giving a deviation from the equilibrium state.

Next, we obtain non-uniform eigenstates which are orthogonal to the uniform eigenstates obtained above. Then, we consider states satisfying the following relations:

$$\sum_{i=1}^{n_{\rm HS}} p_i = 0, \quad \sum_{j=n_{\rm HS}+1}^{n=n_{\rm HS}+n_{\rm LS}} q_i = 0, \tag{42}$$

i.e., eigenvectors of the forms:

$$\begin{pmatrix} p_1 \\ p_2 \\ \vdots \\ p_{n_{\rm HS}} \\ 0 \\ \vdots \\ 0 \end{pmatrix}, \quad \text{and} \quad \begin{pmatrix} 0 \\ 0 \\ \vdots \\ 0 \\ q_1 \\ \vdots \\ q_{n_{\rm LS}} \end{pmatrix}. \tag{43}$$

The operation for the upper part (of HS states) is given by

$$\begin{pmatrix} \alpha & \beta & \cdots & \beta \\ \beta & \ddots & \cdots & \beta \\ \vdots & \vdots & \ddots & \vdots \\ \beta & \cdots & \cdots & \alpha \end{pmatrix} \begin{pmatrix} p_1 \\ p_2 \\ \vdots \\ p_{n_{\rm HS}} \end{pmatrix} = (\alpha - \beta) \begin{pmatrix} p_1 \\ p_2 \\ \vdots \\ p_{n_{\rm HS}} \end{pmatrix}, \tag{44}$$

where we used the condition $\sum_{i=1}^{n_{\rm HS}} p_i = 0$. Thus, the eigenvalues are $(n_{\rm HS}-1)$-fold degenerate to be

$$\lambda = \alpha - \beta = 1 - n_{\rm HS}\beta - n_{\rm LS}\gamma. \tag{45}$$

Similarly, from the lower part, we find $(n_{\rm LS}-1)$-fold degenerate eigenvalues:

$$\lambda = \alpha' - \beta' = 1 - n_{\rm HS}\beta' - n_{\rm LS}\gamma'. \tag{46}$$

Because uniformizations within HS states or within LS states are expected to be fast, i.e., we assume these eigenvalues for non-uniform cases are small. Therefore, the relaxation process the uniform modes with slow relaxation time plays important role.

2. Timescales of the Ising-like model

In this case that the system has only two states ($\sigma = \pm 1$), the time evolution matrix is given by

$$\boldsymbol{P}(t+\Delta t) = \mathcal{L}\boldsymbol{P}(t) = \begin{pmatrix} 1 - w_{\rm HS\to LS}\Delta t & w_{\rm LS\to HS}\Delta t \\ w_{\rm HS\to LS}\Delta t & 1 - w_{\rm LS\to HS}\Delta t \end{pmatrix} \begin{pmatrix} p_{\rm HS} \\ p_{\rm LS} \end{pmatrix}, \tag{47}$$

where

$$w_{\mathrm{HS}\to\mathrm{LS}} = \frac{1}{\tau_0}e^{\beta(D-k_{\mathrm{B}}T\ln g/2)} = \frac{1}{\tau_0}\sqrt{\frac{1}{g}}e^{\beta D} = \frac{1}{\tau_0\sqrt{n_{\mathrm{HS}}n_{\mathrm{LS}}}}n_{\mathrm{LS}}e^{\beta D},$$
$$w_{\mathrm{LS}\to\mathrm{HS}} = \frac{1}{\tau_0}e^{-\beta(D-k_{\mathrm{B}}T\ln g/2)} = \frac{1}{\tau_0}\sqrt{g}e^{-\beta D} = \frac{1}{\tau_0\sqrt{n_{\mathrm{HS}}n_{\mathrm{LS}}}}n_{\mathrm{HS}}e^{-\beta D}. \tag{48}$$

The eigenvalues are obtained by

$$\begin{vmatrix} 1-w_{\mathrm{HS}\to\mathrm{LS}}\Delta t-\lambda & w_{\mathrm{LS}\to\mathrm{HS}}\Delta t \\ w_{\mathrm{HS}\to\mathrm{LS}}\Delta t & 1-w_{\mathrm{LS}\to\mathrm{HS}}\Delta t-\lambda \end{vmatrix} = 0 \to (\lambda-1)(\lambda-(1-w_{\mathrm{HS}\to\mathrm{LS}}-w_{\mathrm{LS}\to\mathrm{HS}})) = 0. \tag{49}$$

as

$$\lambda_0^{\mathrm{Ising-like}} = 1, \quad \lambda_1^{\mathrm{Ising-like}} = 1-w_{\mathrm{HS}\to\mathrm{LS}}\Delta t - w_{\mathrm{LS}\to\mathrm{HS}}\Delta t. \tag{50}$$

The relaxation time is given by

$$(\lambda_1^{\mathrm{Ising-like}})^n = e^{-t/\tau^{\mathrm{Ising-like}}}, \quad t=n\Delta t, \to \frac{1}{\tau^{\mathrm{Ising-like}}} = -\frac{\ln\lambda_1^{\mathrm{Ising-like}}}{\Delta t} \simeq w_{\mathrm{HS}\to\mathrm{LS}}+w_{\mathrm{LS}\to\mathrm{HS}}. \tag{51}$$

Comparing τ for the degenerate model and $\tau^{\mathrm{Ising-like}}$, i.e.,

$$\frac{1}{\tau} = \frac{1}{\tau_{\mathrm{X}}}\left(n_{\mathrm{LS}}e^{\beta D}+n_{\mathrm{HS}}e^{-\beta D}\right), \quad \frac{1}{\tau^{\mathrm{Ising-like}}} = \frac{1}{\tau_0\sqrt{n_{\mathrm{HS}}n_{\mathrm{LS}}}}\left(n_{\mathrm{LS}}e^{\beta D}+n_{\mathrm{HS}}e^{-\beta D}\right), \tag{52}$$

we find that the relaxation times of the Ising-like model and the degeneracy model have the same dependencies on the temperature. Here τ_{X} is a typical time of contacts for each microscopic state s_i with the thermal bath, while $\tau^{\mathrm{Ising-like}}$ is a typical time of contacts for one of HS state and LS state σ_i with the thermal bath. For the overall timescale, they are different by the factor $\tau_0\sqrt{n_{\mathrm{HS}}n_{\mathrm{LS}}}/\tau_{\mathrm{X}}$. But this factor is constant throughout the process and the difference does not affect temperature dependence of the relaxation process. Therefore, we conclude that both models have the same dynamics, and the use of the Ising-like model is verified to study the original degenerate model.

B. Considerations on dynamical effects on the spin conversions

In Sec. II C 2, we considered the two-temperature model to explain the two-step evolution of spin conversions in the rapid uniformization of lattice temperature. We may have a question what the essential role of the two temperatures is, and what physical meaning of the spin temperature is. The answer should be in the timescales of microscopic processes, e.g., energy transfer and spin conversion, and so on.

The two-temperature model suggests the importance of the timescales of processes. Here, we explore some mechanisms which make the elastic step in a rapid uniformization of the temperature in a single-temperature model by modifying the transition probability considering dynamical effects on the spin conversion.

As we discuss above, the dynamics of the spin conversion is not simply given by thermal process which is given by MC simulation with the detailed balance, and we need to consider properies of direct mechanical process. In principle, the latter cannot be taken into account in MC. But below, we try to argue modelings with modifying the transition probability.

Here, we consider the timescales of thermal process and mechanical process. Because of the degeneracy, spin states change not only due to mechanical force (the pressure), but also due to the entropic force due to the difference of degeneracies g. When the mechanical deformation is small, spin conversion takes place as thermal process (Fig. 13(a)), which may be called entropy-driven conversion. Figure 13(a) schematically shows that the effective energy of HS part is lowered by the entropy effect $D-k_{\mathrm{B}}T\ln g/2$ although the energy of HS part itself is higher by D. On the other hand, when the mechanical deformation is large, spin conversion takes place by a mechanical force, e.g., the pressure (Fig. 13(b)), which may be called mechanical-driven conversion. Figure 13(b) schematically shows that HS state is forced to convert to LS state due to large pressure. In this process, heat emission takes place in a short time and the local heat bath may not absorb it immediately.

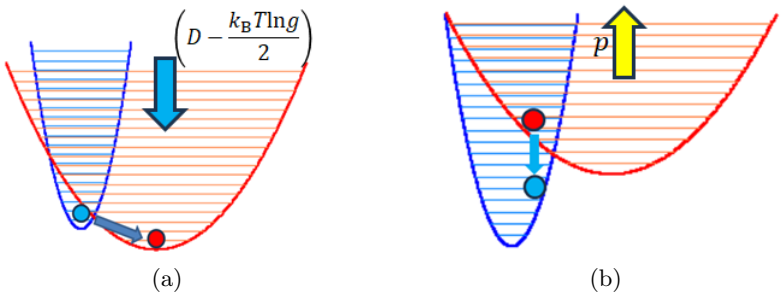

(a) (b)

FIG. 13: (a) Spin conversion caused by the degeneracy difference (entropy-driven conversion), (b) Spin conversion caused by mechanical force (mechanical-driven conversion).

1. *Timescales of thermal process and mechanical process*

We expect the relaxation time for the entropy driven process to be longer than that of mechanical driven processes because the entropic force becomes relevant after many contacts of the heat bath to recognize the degeneracy difference. Although such an effect is difficult to be expressed by a transition probability satisfying the detailed balance, we dare to introduce dependence of the relaxation time as a function of mechanical energy to take into account such aspect approximately and try to find two-step conversion within a single temperature model with fast uniformization of lattice temperature. For example, we may introduce dependence of the relaxation time as a function of mechanical energy.

$$\frac{1}{\tau_0} = \frac{a \tanh\left(\frac{E_{\mathrm{M0}}}{E_0}\right) + b}{a + b}, \tag{53}$$

where E_0 is the total energy and E_{M0} is the mechanical part. a and b are control parameters. By tuning parameters, we may have two steps (not shown), but this choice of transition probability violates the detailed balance. Thus, in principle, the difference of dynamics must be taken into account by a mechanical way but not by the form of transfer probability, which should be an important subject in the future. Some trials of such treatments will be discussed later.

2. *timescales of heat absorption to the local bath in mechanical spin-conversion process*

Next, we consider the timescale of heat flow to the thermal bath in spin conversion. In the master equation approach, the transitions occur in contact with the thermal bath. There, the change of energy in the transition is assumed to be absorbed to the thermal bath immediately. This assumption is good when the bath is very large where exchanges of the energy are done immediately and the temperature of the bath does not change.

However, when we consider the local temperature, the local bath which consists of various modes of a molecule is not so large. Then, it is expected to take some time before the emitted energy is absorbed in the bath. Due to the emitted energy, the local temperature would change in a short time. As a typical case, let us consider the process where the photo-irradiated excited spin is pushed back to LS state due to the high pressure (Fig. 13(b)). In this process, the energy (i.e., heat) is emitted to the local environment (Fig. 14(a)). Therefore, the local lattice temperature increases. We try to reproduce the two-step spin conversion to take the heating due to the emission within the single temperature model with fast uniformization of the temperature.

It is found that, if we take into account temperature increase due to the emission, we can reproduce two steps in a single-temperature model with tuned parameters (at $t = 700$ and 13000 in Fig. 14(b)). When λ is large, the temperature profile becomes homogeneous in an early stage even in the single-temperature model. In Fig. 14(c), the temperature profile at $t = 200$ is depicted.

In this section, we explored possible mechanisms to realize two steps in a single-temperature model taking into account some dynamical mechanisms, and we reproduce two-steps in a single temperature by considering additional effects at photo-excited sites. These results could lead to the hypothesis that the spin-temperature in the two-temperature model may represent the difference types of spin conversion (i.e., mechanical or thermal), or heat emission at the spin-conversion of irradiated molecule. However, more systematic investigations on dynamical effects are necessary.

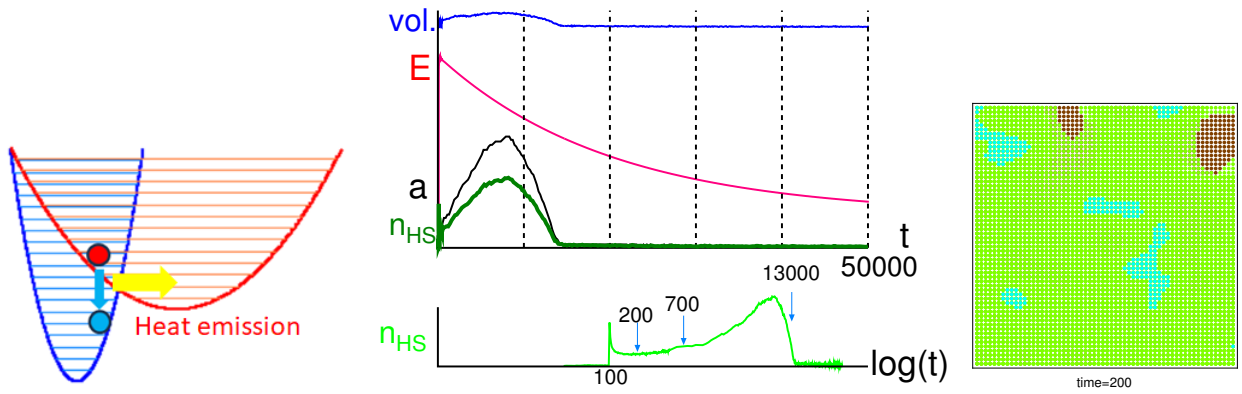

(a) (b) (c)

FIG. 14: (a) Heat emission in the process of compression by the pressure. (b) Two steps in a single-temperature model with tuned parameters taking into account the temperature increases due to compression. Example of two steps in a two-temperature model with $r_H/r_L = 1.1$, $\lambda = 0.02$ and $\kappa = 0.00005$ in a two-dimensional system with 60×60 sites. the notations are the same in Fig. 9. Temperature increase by heat emission is 100K. (c) temperature profile at $t = 200$. The temperature of the irradiated site is $T_{EX} = 400$K, and the probability of irradiated sites is $p = 0.23$.

IV. SUMMARY AND DISCUSSION

In this paper, theoretical models for spin crossover phenomena were reviewed. Characteristics of spin crossover systems are the difference of the degeneracy of the LS and HS states, i.e., n_{HS} and n_{LS}, and the elastic interaction due to the difference of local lattice structure, e.g., the volume of molecules. The former is treated by the Ising-like model [2–4], and the latter is treated by several models taking the elastic energy due to lattice deformation [6–9]. Moreover, to explain the dynamical aspects of ordering processes, such as the two-stage ordering after photo-irradiation (elastic step and thermal step) [19, 20], mechanism of heat (energy) conduction is important. For this point, single-temperature model and the two-temperature model have been introduced. The conventional single-temperature model studied in Sec III C-1 cannot reproduce the two-step transition in a rapid uniformization of temperature found experimentally [22], and the concept of the spin-temperature which is a part of the energy responsible to the spin conversion has been introduced. This two-temperature model succeeded to reproduce the two steps in rapid uniformization of the lattice temperature [21]. The idea of the spin temperature suggests the importance of the timescale of the processes. In the present paper, we studied timescales of the original degenerate model and the Ising-like model. It was found that the relaxation time of both models have the same temperature dependence although the overall factor is different. Thus, it is verified to use the Ising-like model to study dynamics. Moreover, we try to realize the two steps, i.e., the elastic step besides the thermal step in rapid uniformization of the temperature in a single temperature model. We considered some modifications of transition probability, taking into account effects due to the difference of thermal and entropic forces and of local heat emission in the spin-conversion by pressure. It was found that the elastic step appears in such modifications.

For real time phenomena, more investigations of time dependent processes are necessary, which will be important for fast manipulation of spin states by ultrafast pulses. As for the discussion on the timescales related to the thermal exchange between the molecule and its local heat bath, concrete information of intramolecular and intermolecular vibrations and ligand distortions is inevitable. Such microscopic details depend on materials. In the present work, we only discussed the importance of timescales, and the details will be postponed to future studies. Moreover, the present paper does not refer to the microscopic processes of irradiation where the interaction between the electromagnetic field and the spins is important. Such processes are relevant also for general manipulation of quantum systems. Most of works focus on control of spin state [36], but the dynamics with abrupt strong pumping such as the present case of irradiation should be an important issue for the future studies.

Acknowledgments

We would like to thank all the collaborators. The present work was partially supported by JSPS KAKENHI Grant Number JP18K03444. During the preparation of the present paper, one of the authors, our great collaborator and

friend, Cristian Enachescu passed away. We would like to express our gratitude for his essential contribution to this paper and his great achievements in the field of spin transition materials.

Computational Details

Part A: Ising-like model with interaction

The partition function for the system with interactions is given by

$$Z = \sum_{\text{all the states of } s_i} e^{\beta\left(J\sum_{ij} s_i s_j - D\sum_{i=1}^{N} s_i\right)}. \tag{54}$$

We express the Boltzmann factor for each state of $\{s_i\}$ by $\{\sigma_i\}$:

$$e^{\beta\left(J\sum_{ij} s_i s_j - D\sum_{i=1}^{N} s_i\right)} = e^{\beta\left(J\sum_{ij} \sigma_i \sigma_j - D\sum_{i=1}^{N} \sigma_i\right)} \tag{55}$$

Taking the degeneracy of s_i, the partition function is given by

$$Z = \sum_{\text{all the states of } \sigma_i} \prod_{i}^{N} n_i(\sigma_i) e^{\beta\left(J\sum_{ij} \sigma_i \sigma_j - D\sum_{i=1}^{N} \sigma_i\right)}, \tag{56}$$

where $n_i(\sigma_i)$ is $n_{\rm HS}$ when $\sigma_i = 1$ and $n_{\rm LS}$ when $\sigma_i = -1$, which is expressed as

$$n_i(\sigma_i) = \sqrt{n_{\rm HS} n_{\rm LS}} e^{\frac{1}{2}\sigma_i \ln \frac{n_{\rm HS}}{n_{\rm LS}}} = \begin{cases} n_{\rm HS} & \text{for} \quad \sigma_i = 1 \\ n_{\rm LS} & \text{for} \quad \sigma_i = -1 \end{cases} \tag{57}$$

Then, the partition function is given by

$$Z = \sum_{\{\sigma_i = \pm 1\}} e^{\beta\left(J\sum_{ij} \sigma_i \sigma_j - D\sum_{i=1}^{N} \sigma_i\right)} \sqrt{n_{\rm HS} n_{\rm LS}})^N e^{\frac{1}{2}\ln \frac{n_{\rm HS}}{n_{\rm LS}} \sum_{i=1}^{N} \sigma_i}$$

$$= (\sqrt{n_{\rm HS} n_{\rm LS}})^N \sum_{\{\sigma_i = \pm 1\}} e^{\beta\left(J\sum_{ij} \sigma_i \sigma_j + \left(-D + \frac{1}{2} k_{\rm B} T \ln \frac{n_{\rm HS}}{n_{\rm LS}}\right) \sum_{i=1}^{N} \sigma_i\right)}. \tag{58}$$

Thus, the model is regarded as an Ising model with the effective temperature dependent field:

$$H_{\rm eff} = -D + \frac{1}{2} k_{\rm B} T \ln \frac{n_{\rm HS}}{n_{\rm LS}}. \tag{59}$$

For a ferromagnetic model which has a critical temperature $T_{\rm C}$, the system exhibits a first-order phase transition as function of the magnetic field H below the critical point. Thus, the present model exhibits a first order phase transition at $H_{\rm eff} = 0$ if

$$k_{\rm B} T_0 = \frac{2D}{\ln \frac{n_{\rm HS}}{n_{\rm LS}}} < k_{\rm B} T_{\rm C}. \tag{60}$$

Thus, the phase transition occurs when

$$D < \frac{1}{2} k_{\rm B} T_{\rm C} \ln \frac{n_{\rm HS}}{n_{\rm LS}}. \tag{61}$$

Here we do not use any approximation, e.g., the mean-field approximation, and the condition of the first-order phase transition holds generally.

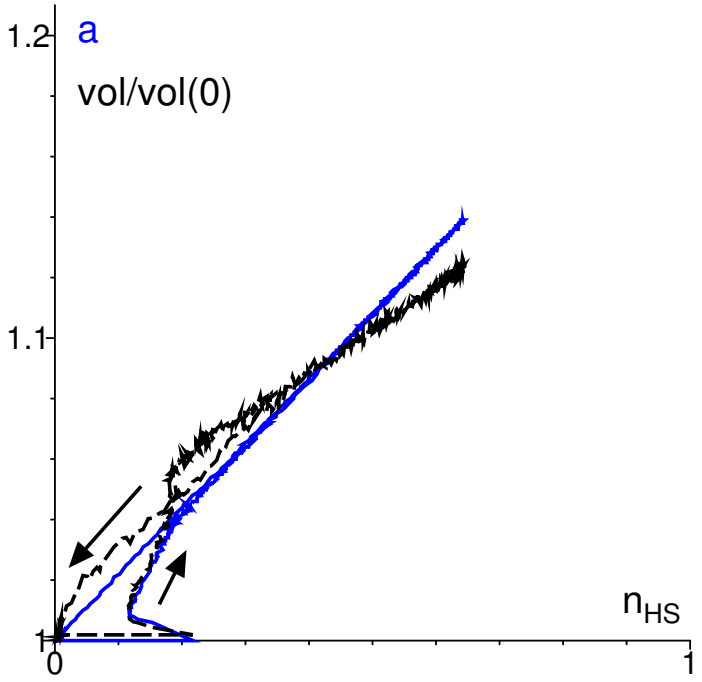

FIG. 15: Plot of a (blue solid line) and vol (black dotted line) vs $n_{\rm HS}$.

Part B: Relations "a" and "vol" vs. "$n_{\rm HS}$"

In Fig. 15, we plot a (blue solid line) and vol (black dotted line) vs. $n_{\rm HS}$. The arrows shows the movements in time. At an early time, $n_{\rm HS}$ shows the elastic step and changes nonmonotonically, while "a" and "vol" change monotonically.

[1] O. Kahn, *Molecular Magnetism* (VCII, 1993), M. A. Halcrow(ed.), *Spin-Crossover Materials*(Wiley, 2013). P. Gütlich and A. Goodwin, *Spin Crossover in Transition Metal Compounds*, Vols. I-III. Topics in Current Chemistry, Vols. **233, 234, 235**. Springer-Verlag, Berlin, Heidelberg, New York (2004). Kamel Boukheddaden; Seiji Miyashita; Smail Triki, J. Appl. Phys. **132**, 220402 (2022).

[2] J. Wajnflasz and J. Pick: Phys (France) **32**, C1-91-C91-92 (1971). A. Bousseksou, J. Nasser, J. Linares, K. Boukheddaden, and F. Varret: J. Phys. I France **2**, 1381 (1992).

[3] S. Miyashita, Y. Konishi, H. Tokoro, M. Nishino,K. Boukheddaden, F. Varret: Prog. Theor. Phys. **114**, 719 (2005).

[4] S. Miyashita, Proceedings of the Japan Academy Series B **86**, (643-666) (2010).

[5] S. Miyashita, *Collapse of Metastability*, Springer-Nature (2022).

[6] M. Nishino, K. Boukheddaden, Y. Konishi, and S. Miyashita, Phys. Rev. Lett. **98**, 247203 (2007). K. Boukheddaden, M. Nishino and S. Miyashita, Phys. Rev. Lett. **100**, 177206 (2008). M. Nishino, K. Boukheddaden and S. Miyashita, Phys. Rev. B **79**, 012409 (1-4) (2009).

[7] Y Konishi, H. Tokoro, M. Nishino and S. Miyashita, Phys. Rev. Lett. **100**, 067206 (1-4) (2008).

[8] C. Enachescu, L. Stoleriu, A. Stancu, and A. Hauser, Phys. Rev. Lett. **102**, 257204 (2009). C. Enachescu, L. Stoleriu, A. Stancu, and A. Hauser, Phys. Rev. B **82**, 104114 (2010).

[9] C. Enachescu, M. Nishino, S. Miyashita, K. Boukheddaden, F. Varret, and P. A. Rikvold, Phys. Rev. B **91**, 104102 (2015).

[10] S. Miyashita, Y. Konishi, M. Nishino, H. Tokoro and P.A. Rikvold, Phys. Rev. B **77**, 0144105 (2008).

[11] M. Nishino, C. Enachescu, S. Miyashita, P. A. Rikvold, K. Boukheddaden, and F. Varret, Sci. Rep. **1**, 162 (2011).

[12] M. Nishino, T. Nakada, C. Enachescu, K. Boukheddaden, and S. Miyashita, Phys. Rev. B **88**, 094303 (2013).

[13] A. Slimani, K. Boukheddaden, F. Varret, H. Oubouchou, M. Nishino and S. Miyashita, Phys. Rev. B **87**, 014111 (2013), A. Slimani, K. Boukheddaden, F. Varret, M. Nishino and S. Miyashita, J. Chem. Phys. **139**, 194706 (2013).

[14] T. Nakada, T. Mori, S. Miyashita, M. Nishino, S. Todo, W. Nicolazzai and P. A. Rikvold, Phys. Rev. B **85**, 054408(1-8) (2012).

[15] P. A. Rikvold, G. Brown, S. Miyashita, C. Omand, and M. Nishino, Phys. Rev. B **93**, 064109 (2016). C. H. Chan, G. Brown, and P. A. Rikvold, Phys. Rev. E **95**, 053302 (2017), Phys. Rev. B **96**, 174428 (2017). M. Nishino, S. Miyashita, and P. A. Rikvold, Phys. Rev. B **96**, 144425 (2017). M. Nishino, P. A. Rikvold, C. Omand, and S. Miyashita, Phys. Rev. B **98**, 144402 (2018).

[16] Yogendra Singh, Hassane Oubouchou, Masamichi Nishino, Seiji Miyashita, and Kamel Boukheddaden, Phys. Rev. B **101**, 054105 (1-15) (2020).

[17] Masamichi Nishino, Cristian Enachescu, and Seiji Miyashita, Phys. Rev. B **100**, 134414 (2019). M. Nishino, Y. Singh, K. Boukheddaden, and S. Miyashita, Tutorial on elastic interaction models for multistep spin-crossover transitions, J. Appl. Phys. **130**, 141102 (2021).

[18] Y. Hu, M. Picher, N. M. Tran, M. Palluel, L. Stoleriu, N. Daro, S. Mornet, C. Enachescu, E. Freysz, F. Banhart, G. Chastanet, Adv. Materials **33**, 2105586 (2021).

[19] R. Bertoni, M. Lorenc, H. Cailleau, A. Tissot, J. Laisney, M. Boillot, L. Stoleriu, A. Stancu, C. Enachescu, and E. Collet, Nat. Mater. **15**, 606 (2016).

[20] C. Enachescu, L. Stoleriu, M. Nishino, S. Miyashita,3 A. Stancu, M. Lorenc, R. Bertoni, H. Cailleau, and E. Collet, Phys. Rev. B **95**, 224107 (2017).

[21] Laurentiu Stoleriu, Masamichi Nishino, Seiji Miyashita, Alexandru Stancu, Roman Bertoni, Eric Collet, Maciej Lorenc, and Cristian Enachescu, Phys. Rev. B **108**, 014306(1-11) (2023).

[22] H. Cailleau, M. Lorenc, L. Guerin, M. Servol, E. Collet, and M. Buron-Le Cointe, Acta Crystallogr A Found Crystallogr. **66**, 189 (2010).

[23] M. Sorai and S. Seki, J. Phys. Chem. Solids, **35**, 555 (1974), M. Sorai, Bull. Chem. Soc. Jpn. **74**, 2223 (2001).

[24] M. Nishino, S. Miyashita and K. Boukheddaden, J. Chem. Phys. **118**, 4594-4597 (2003).

[25] S. Miyashita and N. Kojima, Prog. Theor. Phys. **109**, 729-739 (2003).

[26] S. Zerdane, L.Wilbraham, M. Cammarata, O. Iasco, E. Riviere, M. L. Boillot, I. Ciofini, and E. Collet, Chem. Sci. **8**, 4978 (2017). A. Marino, P. Chakraborty, M. Servol, M. Lorenc, E. Collet, and A. Hauser, Angew. Chem. Int. Ed. **53**, 3863 (2014). S. Decurtins, P. Gütlich, C. P. Kohler, H. Spiering, and A. Hauser, Chem. Phys. Lett. **105**, 1 (1984). A. Hauser, Top. Curr. Chem. **234**, 155 (2004).

[27] Y. Konishi, H. Tokoro, M. Nishino and S. Miyashita, J. Phys. Soc. Jan. **75**, 114603 1-9 (2006).

[28] H. Tokoro, S. Miyashita, K. Hashimoto, and S. Ohkoshi, Phys. Rev. B**73**, 172415 (2006).

[29] H. Tokoro and S. Ohkoshi, Appl. Phys. Lett., **93**, 021906 (2008).

[30] M. Nishino and S. Miyashita, Phys. Rev. B **88**, 014108 (1-14) (2013).

[31] N. Bréfuel, H. Watanabe, L. Toupet, J. Come, M. Kojima, N. Matsumoto, E. Collet, K. Tanaka, and J. P. Tuchagues, Ang. Chem. Int. Ed **48**, 9304 (2009). H. Watanabe, K. Tanaka, N. Brefuel, H. Cailleau, J. F. Letard, S. Ravy, P. Fertey, M. Nishino, S. Miyashita and E. Collet, Phys. Rev. B **93**, 014419 (2016).

[32] N. Willenbacher and H. Spiering, J. Phys. C **21**, 1423 (1988). H. Spiering and N. Willenbacher, J. Phys.: Condens. Matter **1**, 10089 (1989). H. Spiering, Top. Curr. Chem. **235**, 171 (2004).

[33] S. Nosé, J. Chem. Phys. **81**, 511 (1984). W. G. Hoover, Phys. Rev. A **31**, 1695 (1985).

[34] C. Enachescu and W. Nicolazzi, Comptes Rendus Chimie **21**, 1179 (2018).

[35] M. Nishino and S. Miyashita, Phys. Rev. B **91**, 134411(1-13) (2015).

[36] S. Miyashita, T. Shirai, T. Mori, H. De Raedt, S. Bertaina and I. Chiorescu,, J. Phys. B Atomic Mol and Opt Phys, **45**, 124010 (2012). T. Shirai, S. Todo, H. De Raedt, and S. Miyashita, Phys. Rev. A**98**, 043802 (2018). N. Lambert, et al., Phys. Rev. Research **5**, 013181 (2023), and X. Wang et al. AVS Quantum Sci. **5**, 043801 (2023).